UNIVERSAL WISER
PUBLISHER

Research Article

Forecasting-Aided State Estimation in Power Systems during Normal Load Variations Using Iterated Square-Root Cubature Kalman Filter

Teena Johnson[*] , **Sofia Banu** and **Tukaram Moger**

Department of Electrical & Electronics Engineering, National Institute of Technology Karnataka, Surathkal, Mangalore, India
E-mail: teenaj2007@gmail.com

Abstract: The main aim is to estimating the voltage profile at all the buses in the system before the arrival of next set of hybrid measurements from field. The effectiveness of the algorithm ISCKF during load variations is evaluated with respect to already implemented Kalman filter approaches for this application. This includes the sudden changes in loads which occurring in practical power systems. The utilization of an iterated square-root cubature Kalman filter (ISCKF) for power system forecasting-aided state estimation (FASE) is being studied during normal load variations. Its implementation involves "Newton-Gauss iterative method being embedded into the square-root cubature Kalman filter (SCKF)" at the measurement update step of Kalman filter. The square-root factor of error covariance matrices is calculated by utilizing QR decomposition to avoid losing of positive definiteness of the matrix. The estimation is carried out utilizing hybrid measurements from remote terminal units and phasor measurement units. The state vector is forecasted using the proposed method in the interval period between two measurement arrivals from the devices. Thereby, caters to state estimation of the voltages at buses in the system even when the measurements are unavailable. The efficacy of the proposed algorithm to FASE is evaluated for IEEE 30-bus system and Northern Region Power Grid (NRPG) 246-bus system. The simulation results show that the proposed ISCKF outperforms the CKF by significant improvement in accuracy of forecasting-aided state estimation. ISCKF will be able to give results before the next set of hybrid data arrives (expected from an estimation algorithm). Therefore, the proposed estimation algorithm is applicable for real-time practical application, with respect to large power systems as well.

Keywords: forecasting-aided state estimation (FASE), bayesian estimation, voltage profile tracking, iterated square-root cubature kalman filter

1. Introduction

State estimating process for power network has been traditionally described as a static estimate issue, solved using weighted least square (WLS) technique. In this work, state estimation implementation involves "Newton-Gauss iterative method [1] being embedded into the square-root cubature Kalman filter (SCKF)" at the measurement update step of Kalman filter. With the advent of wide area measurement systems, hybrid state estimation algorithms were created by adapting the traditional WLS technique to include phasor measurement units (PMU) measurements [2, 3, 4, 5, 6]. The PMU and remote terminal unit (RTU) measurements are combined to generate the augmented measurement set [2, 3]. As a result, the Jacobian matrix is changed in order to run the WLS-based static state estimation (SE). The WLS method is utilized

only for RTU data, and later the PMU data and the SE results were used together to perform the linear SE [4]. PMU current measurements are used to run the hybrid state estimation [6]. In the literature, a few different versions of the WLS technique [7], have been used for SE. The Jacobian matrix grows in size as the PMU measurements are included in the hybrid state estimation execution. As a result, the SE's execution time increases. Furthermore, the current SSE technique does not allow for the use of all relevant metrics in predicting states. As a result, a quick SE technique is needed, one that can use both RTU and PMU data to estimate states before the next set of measurement data arrives.

The main steps involved in the implementation for FASE methodology involves:

- System state model identification

- State prediction using a forecasting tool

- State filtering

For power system dynamic SE studies until 2017 [8], the systems were assumed to be in quasi steady state and hence load variations were considered to be slow. Sudden changes in loads were not considered. Now in our work here, the effectiveness of the proposed algorithm taking "load variations" into account is demonstrated. In this case, the resulting estimators are referred to as FASE [9]. Power system state estimation consists of a multi-level extended Kalman filter whose time-update step uses a dynamic load prediction method, and whose measurement update step uses a hierarchical technique [10]. It is observed that load forecasting and DSE are complementary to one another.

In another attempt, for estimation of both fundamental and harmonic components of voltage magnitude and angles of a power system, Kalman filter has been employed effectively [11]. It is presented how load fluctuations impact the power system's harmonics. An artificial neural network (ANN) based short-term load forecasting is employed for the prediction step in DSE because to its quick response and effective learning [12]. Similarly deep learning has been explored for distribution system FASE [13]. But, for all machine learning techniques a huge amount of training dataset need to be provided for high precision. To address state estimation uncertainties, DSE with a fuzzy logic controller that is improved by the sliding surface concept is examined [14].

Kalman filter-based algorithms appear to dominate the DSE in power systems [15], whereas for the state prediction step, ANN, fuzzy logic, autoregression, Box, and Jenkins approaches have been investigated in the literature. The nonlinearity of the measurement function is addressed by [16] but this method has non-sparse measurement covariance matrix and hence requires large computational time. To overcome this drawback, a two-level estimation is proposed by [17]. Square root KF is more robust but algebraically identical to KF [18]. Square root KF reduces uncertainty in measured data, saving time and computational memory when compared to KF.

Utilization of synchrophasor data in state estimation [19] is advantageous as with high accuracy angle measurements and convergence speed increases. For the state prediction stage, Holt's double exponential smoothing is adopted, while EKF is utilised for the filtering stage. For DSE, an adaptive EKF is assessed under normal, bad data, and rapid load fluctuations conditions [20]. Adaptive EKF has the best filtering performance when compared to standard EKF. However, the processing time is little longer. To deal with certain missing measurement data owing to communication loss, a time-forward Kriging model depending on a load forecasting technique was incorporated in DSE [21]. Unscented KF being an easier and derivative-free implementation is applied for DSE [22]. Projected UKF [23] is proposed for DSE using unscented transformation and zero injection constraints. It performed better in FASE than that of EKF or UKF. Regression analysis based state transition matrix is proposed for enhanced dynamic SE [24]. A combination of both differential evolution and bacteria foraging, is employed for the filtering stage in [25]. Furthermore, in the forecasting step, a novel stochastic search technique and Lattice Monte Carlo method is utilized. In distribution systems for carrying out FASE, there is inadequacy in quantity of real-time data readings [13]. Even though many smart meters are installed, their low data reporting rate when compared to RTU or PMU data and unable to estimate within the execution time as expected. A robust UKF algorithm based on generalized maximum mixture correntropy criterion is proposed for FASE in [26] which showed better accuracy and robustness compared to traditional correntropy algorithms. In the further study, to incorporate the influence of gross errors on SE, an adaptive UKF method is adopted in [27]. It estimates the gross errors in measurements to compensate during the intermediate step, so these compensated measurements are used for the corrected state estimation

step. But, when a dynamic process of variations in the power system is close to the stable value, the numerical stability of this method is poor. Another research work [28], explores the online state estimation for distribution grid for anomaly detection, discrimination and identification using EKF method with help real-time digital simulator. The errors contained in the network parameters are not considered in the study due to the complexity to deal with it. Hence, the main challenge would be extend their anomaly detection and identification technique when there are topology changes. Probabilistic forecasting was utilized for dealing with false data injection attacks in distribution grids [29]. While the method performs reasonably well taking only few seconds more than the traditional multi-area deterministic SE method, it is also does not guarantee performance when communication system fails or cyber attack on topology data.

In [8], the Cubature Kalman Filter (CKF) proposed in [30] which employs a more precise cubature process for numerically computing Gaussian-weighted integrals is used for estimating the states in power system. CKF requires the error covariance matrix to be positive definite in every update to avoid stopping the CKF from carry on with its iterations. In [31] ISCKF is explored for space target tracking problem in surveillance systems and is proven to perform better than traditional filters. Contributions of this work are briefed as follows:

1. The ISCKF proposed in [31] is applied for FASE in power systems. Here, the estimation of voltage magnitude and phase angle at all buses is carried out. The robustness of the said technique is ensured by removal of outliers by anticipating measurement data and inherent feature of Kalman filter's resilience against noise in data.

2. Performance of the ISCKF method for voltage profile estimation during load variations is compared with that of the CKF method in terms of estimation error and computation time by the simulation studies. Motivation for the study is to evaluate the presented method which assures high accuracy is capable of a feasible online real-time application.

3. The efficiency and scalability of the ISCKF method application for the FASE is tested using two different sized test systems. The performance is evaluated using two parameters error and estimation time. The error is calculated by finding mean of absolute error between estimated values and actual values.

The paper is made up of the following structure. The power system model for FASE is defined in Section 2. The ISCKF algorithm is described in Section 3. The Section 4 elaborates on how actual data is simulated for carrying out the case studies with the test systems. Section 5 describes what are the case studies carried out. The findings are concluded in Section 6 by comparing the efficiency of the proposed state estimation algorithm with the existing KF-based algorithms.

2. Power system modelling for forecasting-aided state estimation

The linear state transition model for power system and measurements is represented as discrete time functions using difference equations:

$$x_t = f(x_{t-1} - 1) + w_{t-1} \tag{1}$$

$$z_t = h(x_t) + v_t \tag{2}$$

$$w_{t-1} = N(0, \Omega_{t-1}) \tag{3}$$

$$v_t = N(0, R_t) \tag{4}$$

where x_t—state vector at t^{th} time instant, z_t—measurement vector, w_{t-1}—Gaussian process noise with mean of zero and covariance of Ω_{t-1}, v_t—Gaussian and Cauchy measurement noises with mean of zero and covariance of R_t, $f()$ and $h()$—state space and measurement space non-linear functions respectively. Different type of measurements and corresponding standard uncertainties, considered in our study, are shown in Appendix. These standard uncertainties are employed to create the simulated measurement data from the actual data for the simulation studies.

The state vector x_t in the FASE formulation is made up of voltage magnitude (V_t) and voltage angle (θ_t) state sub-vectors. The measurements sub-vectors of voltage magnitude (V_{mt}), real power injection (P_{tm}), reactive power injection (Q_{tm}), real power flow (PF_{tm}), and reactive power flow (QF_{tm}) and voltage angle (θ_{tm}) make up the measurement vector z_t at t^{th} instant as follows:

$$x_t = [V_t \,|\, \theta_t]^T \tag{5}$$

$$z_t = [V_{tm} \,|\, P_{tm} \,|\, Q_{tm} \,|\, PF_{tm} \,|\, QF_{tm} \,|\, \theta_{tm}]^T \tag{6}$$

where the subscript m denotes the quantities measured.

The assumption for the power system transition modeling is that the variations in network characteristics, such as load fluctuations, are sluggish. Quick variations in the states are not taken into account in the current situation. With respect to this assumption, some state forecasting tool [32] could be used for modeling the state transition function and account for the shift in state values from a particular time instant to another. The error in forecasted state can be modelled using a process noise w.

$$f(x_t) = a_{t-1} + b_{t-1} \tag{7}$$

where

$$a_{t-1} = ax_{t-1} + (1-\alpha)x_{t-1}^- \tag{8}$$

$$b_{t-1} = \beta(a_{t-1} - a_{t-2}) + (1-\beta)b_{t-2} \tag{9}$$

where α and β—parameters having values in (0,1), x_{t-1}—forecasted state vector, and a_{t-1} and b_{t-1}—defined by (8) and (9) at $(t-1)^{th}$ instant. When using the KF technique to perform the state predicting phase, the expression (7) is used in (1).

The measurement function $h()$ of the network, uses the well-known P and Q power injections as well as flow expressions, written as [33]:

$$P_j = \sum_{k=1}^{N} |V_j| |V_k| \left(G_{jk} \cos \theta_{jk} + B_{jk} \sin \theta_{jk} \right) \tag{10}$$

$$Q_j = \sum_{k=1}^{N} |V_j| |V_k| \left(G_{jk} \sin \theta_{jk} + B_{jk} \cos \theta_{jk} \right) \tag{11}$$

$$P_{jk} = V_j^2 \left(G_{sj} + G_{jk} \right) - |V_j| |V_k| \left(G_{jk} \cos \theta_{jk} + B_{jk} \sin \theta_{jk} \right) \tag{12}$$

$$Q_{jk} = -V_j^2 \left(B_{sj} + B_{jk} \right) - |V_j| |V_k| \left(G_{jk} \sin \theta_{jk} + B_{jk} \cos \theta_{jk} \right) \tag{13}$$

where P_j—real power injection at bus j, Q_j—reactive power injection at bus j, P_{jk}—real power flow in line j–k, Q_{jk}—reactive power flow in line j–k, V_j—voltage magnitude at bus j, G_{jk}—conductance of line j–k, B_{jk}—susceptance of line j–k, G_s—conductance of shunt at bus j, and B_{sj}—susceptance of shunt at bus j.

Using this power system model the proposed approach is simulated to estimate the states, the voltage magnitude and phase angles at all the buses for the test systems.

3. Iterated square-root cubature kalman filter (ISCKF)

The ISCKF technique is expected to have an increased filtering capability in terms of accuracy and numerical stability, This is due to the fact that its implementation involves Newton-Gauss iterative method [1] being embedded into the square-root cubature Kalman filter (SCKF).

3.1 *Steps to implement ISCKF algorithm for FASE*

3.1.1 *Forecasting step*

At this step, the state vector (Refer (5)) is forecasted based on the estimated state vector from the previous iteration and using the forecasting tool: Holt's double exponential method [32] as described in (7).

1. Assuming initial flat start voltage profile and state covariance matrix is considered as $1 \times 10^{-3} \times I$ initially.

2. Cubature points are derived for the state vector given by:

$$X_{i,k-1|t-1} = S_{t-1|t-1}\, \xi_i + \hat{x}_{t-1|t-1} \quad i = 1, 2, ..., m \tag{14}$$

where, $m = 2n$ and $k = 1$

$$S_{0|0} = sqrt\,(P_0) \tag{15}$$

3. Evaluate cubature points ($i = 1, 2, ..., m$) with the help of $f()$ in (7)

$$X^*_{i,k-1|t-1} = f\left(X_{i,k-1|t-1}\right) \tag{16}$$

4. Estimate predicted state

$$\hat{x}_{t|t-1} = \frac{1}{m}\sum_{i=1}^{m} X^*_{i,t|t-1} \tag{17}$$

5. Now, computing a square-root of the predicted error covariance

$$S_{t|t-1} = Tria\left(\left[x^*_{t|t-1}, S_{Q,t-1}\right]\right) \tag{18}$$

where $Tria(.)$ denotes QR decomposition and $S_{Q,t-1}$ is square-root of Q_{t-1} and, such that $Q = S_{Q,t-1}\, S^T_{Q,t-1}$, and $x^*_{t|t-1}$ defined as

$$x^*_{t|t-1} = \frac{1}{\sqrt{m}}\left[X^*_{1,t|t-1} - \hat{x}_{t|t-1}, X^*_{2,t|t-1} - \hat{x}_{t|t-1}, ..., X^*_{m,t|t-1} - \hat{x}_{t|t-1}\right] \tag{19}$$

3.1.2 *Filtering step*

Here, based on the measurements for time instant k and the forecasted state vector, the Kalman gain is calculated and filtered state vector is derived. This is done recursively for iterations $p = 0, 1, ..., N_{iter}$ where $N_{iter} = 2$ in our study, to get even better filtering effect.

6. Evaluate cubature points ($i = 1, 2, ..., m$) for filtering step,

$$X^{(p)}_{i,k-1|t-1} = \hat{S}^{(p)}_{t-1|t-1}\, \varsigma_i + \hat{x}^{(p)}_{t|t-1} \tag{20}$$

where internal iteration count $j = 0, 1, ..., N_{iter}$ for the filtering step $j = 0$, $\hat{S}^{(0)}_{t|t-1} = S_{t|t-1}$ and $\hat{x}^{(0)}_{t|t-1} = \hat{x}_{t|t-1}$.

7. Evaluate propagated cubature points

$$Z_{i,t|t-1}^{(p)} = h\left(X_{i,t|t-1}^{(p)}\right) \tag{21}$$

8. Calculating the predicted measurement

$$\hat{z}_{t|t-1}\,(p) = \frac{1}{m}\sum_{i=1}^{m} Z_{i,t|t-1}^{(p)} \tag{22}$$

9. Determine square-root of innovation covariance matrix

$$S_{zz,t|t-1}^{(p)} = Tria\left(\left[Z_{t|t-1}^{(p)}\,(p),S_{R,t}^{(p)}\right]\right) \tag{23}$$

where $S_{R,t}^{(p)}-$ square-root factor of $R_t^{(p)}$ in order for $R_t^{(p)} = S_{R,t}^{(p)}\left(S_{R,t}^{(p)}\right)^T$ and $Z_{t|t-1}^{(p)}$ is defined as

$$Z_{t|t-1}^{(p)} = \frac{1}{\sqrt{m}}\left[Z_{1,t|t-1}^{(p)} - \hat{z}_{t|t-1}^{(p)},Z_{2,t|t-1}^{(p)} - \hat{z}_{t|t-1}^{(p)},...,Z_{m,t|t-1}^{(p)} - \hat{z}_{t|t-1}^{(p)}\right] \tag{24}$$

10. Estimate the cross-covariance matrix

$$P_{xz,t|t-1}^{(p)} = X_{t|t-1}^{(p)}\left(Z_{t|t-1}^{(p)}\right)^T \tag{25}$$

where $X_{t|t-1}$ is:

$$X_{t|t-1}^{(p)} = \frac{1}{\sqrt{m}}\left[X_{1,t|t-1}^{(p)} - \hat{x}_{t|t-1}^{(p)},X_{2,t|t-1}^{(p)} - \hat{x}_{t|t-1}^{(p)},...,X_{m,t|t-1}^{(p)} - \hat{x}_{t|t-1}^{(p)}\right] \tag{26}$$

11. Estimate the Kalman gain

$$P_{zz,t|t-1}^{(p)} = S_{zz,t|t-1}^{(p)}\left(S_{zz,t|t-1}^{(p)}\right)^T \tag{27}$$

$$W_t^{(p)} = \frac{P_{xz,t|t-1}^{(p)}}{P_{zz,t|t-1}^{(p)} + R_t^{(p)}} \tag{28}$$

12. Estimate the filtered state

$$\hat{x}_{t|t}^{(p)} = \hat{x}_{t-1|t}^{(p)} + W_t^{(p)}\left(z_t^{(p)} - \hat{z}_{t|t-1}^{(p)}\right) \tag{29}$$

13. Calculate square-root of error covariance

$$S_{t|t}^{(p)} = Tria\left(\left[\chi_{t|t-1}^{(p)} - W_t^{(p)}Z_{t|t-1}^{(p)},W_t^{(p)}S_{R,t}^{(p)}\right]\right) \tag{30}$$

14. Make $\hat{x}_{t|t-1}^{(j+1)} = \hat{x}_{t|t}^{(p)}$, $\hat{S}_{t|t-1}^{(j+1)} = \hat{S}_{t|t}^{(p)}$ and $j = j+1$.

Return to Step 6 and end for $j = N_{iter}$.

4. Simulation of actual data

For the implementation of ISCKF-based FASE approach, the hybrid measurements from both PMUs and RTUs are augmented. We consider the assumption that, for the 50 Hz power system, the PMU data arrive at the rate 25 frames/s (i.e., after every 40 ms), and the RTU data arrive after every 2 s. To simulate the hybrid measurement data for the FASE application, the actual values of the variables that constitute the system states are derived using load flow computations recursively for different simulated varying load conditions. Power flow is run with the help of MATPOWER package

[34] on MATLAB R2020a platform. All the loads are varied in each time step upto ±5% from the values of their prior time-steps during the simulation period. Thus, simulating a realistic load profile. The higher and lower limitations applied in variations of loads throughout time of simulation studies are specified at ±30% of its respective nominal load values. The measurement data are then chosen at random from the normal probability distribution of actual state values acquired from power flow results at different instants. The probability distribution depends on the standard uncertainty as listed in Appendix.

5. Case studies on FASE for test systems

The forecasting-aided state estimation is performed on the test systems with 100 hybrid measurements simulations under varying loading situations using MATLAB R2020a platform. In the 2 s gap across arrival times of two successive RTU data and 49 PMU data measurements (Initial set of PMU data is considered to overlap with that of RTU data) are analysed as well. Hence, overall 4951 (99 × 49 + 100) simulations are carried out to execute the ISCKF technique. The parameters α and β of the forecasting tool are derived by 20,000 Monte Carlo simulations (MCS) [8]. This mainly takes into account the randomness in the measurement data. The MC simulation has been performed off-line, only once before the FASE simulation begins, so as to assess the values of α and β. The following are the test systems considered for the analysis:

5.1 *IEEE 30-bus system*

The single line diagram of the IEEE 30-bus system is shown in Figure 1 (refer [35] for the system details). The α and β derived for this system are 0.76 and 0.53 respectively [8]. For this system, 3 PMUs are chosen to be placed on buses 6, 9 and 12. While the remaining buses are assumed to be placed with RTUs for the data acquisition.
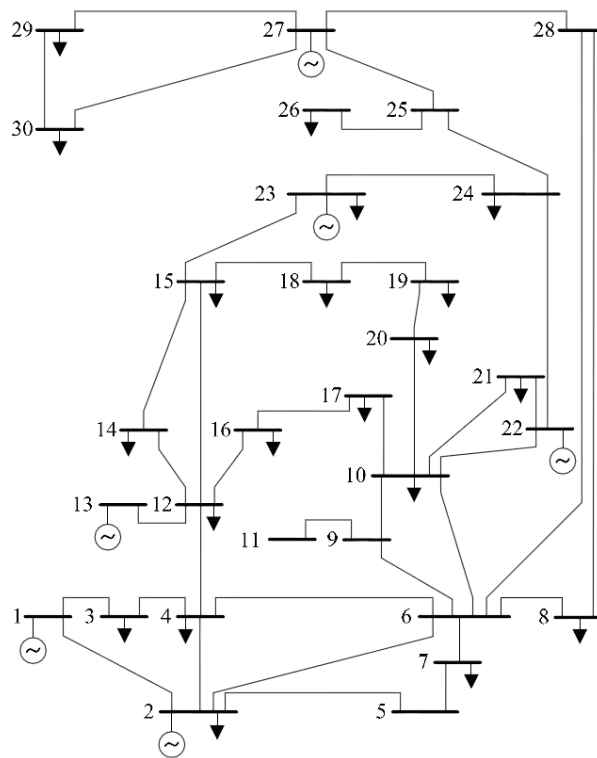

Figure 1. Single line diagram of the IEEE 30-bus system.

5.2 *Northern region power grid (NRPG) 246-bus test system*

Around 30 PMUs are chosen for this system and they are assumed to be installed on huge generator buses. Remaining buses are expected to be connected to RTUs for data collection. Values of α and β derived for NRPG 246-bus system (See Figure 2 and refer [36] for system details) are obtained as 0.83 and 0.64, respectively [8].
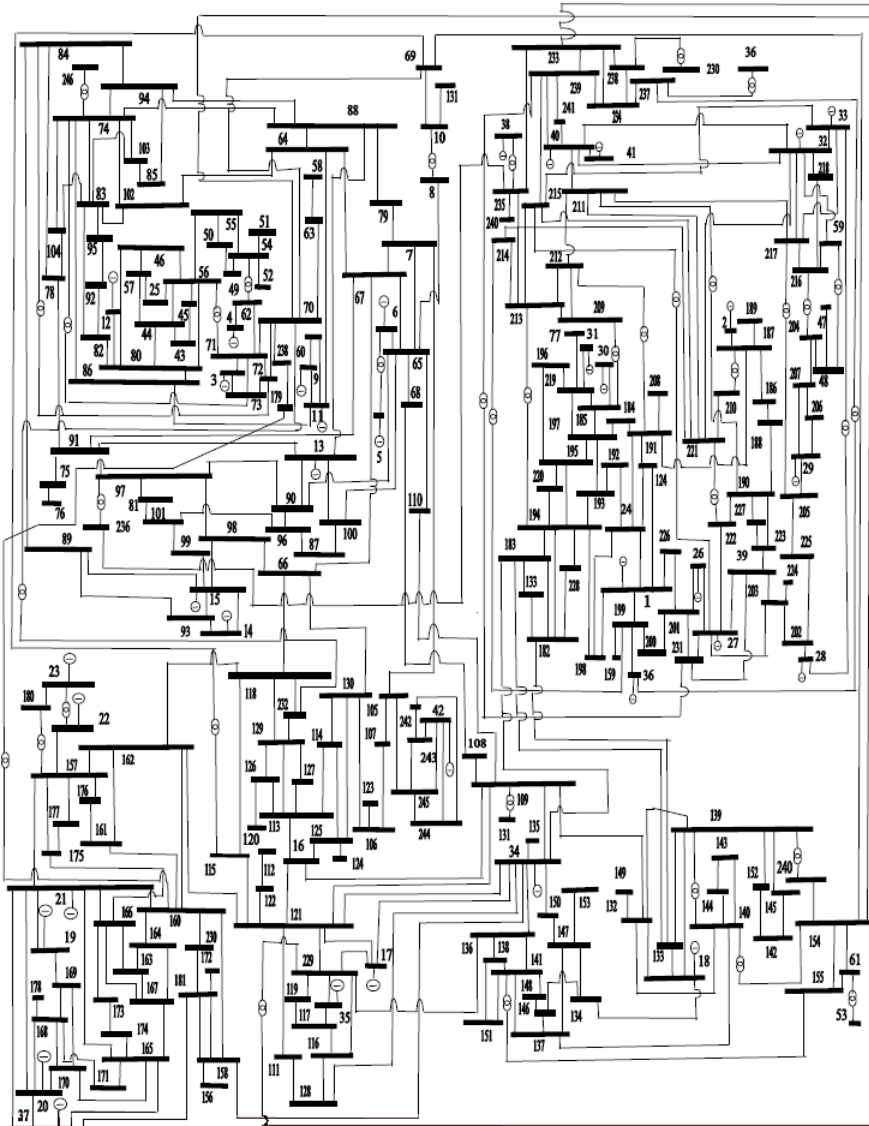

Figure 2. Single line diagram of the NRPG 246-bus system.

6. Results and discussion

The ISCKF based FASE is implemented using 100 hybrid (PMU and RTU) measurements with 49 PMU measurements between each successive RTU measurements. Suppose the proposed FASE begins, at the time step T = 0, by estimating the states with the help of immediately accessible hybrid measurements. Further, utilizing the state estimation outcome for the measurements at T = 0, at the time instant T = 1 (i.e., at 40 ms), the estimate results are forecasted. Now, the combination of these forecasted states as pseudo data and the PMU data accessible at T = 1, derives estimated state variables at T = 1.

These steps are carried out for every PMU measurement set received in the interval between the time steps T = 0 and T = 50. At T = 50 (i.e., at 2 s), when the second batch of RTU data comes, the state is recalculated using the hybrid measurements. The simulation studies are performed using Intel Core-i7 3.4 GHz computer having 32 GB RAM and Windows 10 OS.

For the test systems in the study, the measurement data was simulated by adding noises to the actual data with the standard measurement uncertainty of the devices (See Appendix) at each iteration, to ensure that the simulation findings are consistent. The voltage phasors were added with White Gaussian noises randomly, while Cauchy noises are added to the power measurements. Subsequently, the mean of absolute errors (MAE) for state estimates in each iteration are noted down. By estimating the voltage magnitude and phase angle at all buses in the test systems, the mean of the absolute errors at all buses are compared in the Tables 1 and 2. The speed of an algorithm can be measured by the capability of an algorithm to keep up with the speed of inflowing data. The execution times have been noted down in Table 3 for the systems using CKF and ISCKF for immediate comparison.

Table 1. Mean of Absolute Errors (MAE) in the Estimated States using various KF algorithms for IEEE 30-bus test system.

Filter Type	MAE in V Magnitude (p.u.)	MAE in V Angle (rad.)
ISCKF	0.854×10^{-3}	1.7×10^{-3}
CKF [8]	3.9×10^{-3}	3.3×10^{-3}
UKF [8]	4.2×10^{-3}	4.9×10^{-3}
EKF [8]	4.4×10^{-3}	4.7×10^{-3}

Table 2. Mean of Absolute Errors (MAE) in the Estimated States using various Kalman filter (KF) based algorithms for NRPG 246-bus test system.

Filter Type	MAE in V Magnitude (p.u.)	MAE in V Angle (rad.)
ISCKF	1.8×10^{-4}	2.0×10^{-4}
CKF [8]	2.8×10^{-3}	2.1×10^{-3}
UKF [8]	4.8×10^{-3}	3.9×10^{-3}
EKF [8]	5.8×10^{-3}	6.2×10^{-3}

Table 3. Total computational time for estimation using one set of hybrid measurements and 49 PMU measurements.

	Estimation Time IEEE 30-Bus System	Estimation Time NRPG 246-Bus System
CKF	7.43 ms	0.84 s
ISCKF	15.93 ms	1.36 s

Some important inferences from the results are discussed below:

1. IEEE 30-bus system:

- For the comparison of ISCKF and CKF estimation results, actual data and estimation results for bus voltage plots and their corresponding error plots at bus-7 are shown in Figure 3. From Figure 3b,d, it is inferred that the error in estimation using ISCKF is significantly less than that of using CKF.

- Error in estimation: (a) Mean of absolute error given by: From the mean of absolute errors tabulated in the Table 1 it is noticed that by using ISCKF the Mean absolute error in the voltage magnitude estimation is decreased to 1/5th the error that obtained using CKF. That is, the precision in the voltage magnitude estimation by ISCKF has been improved by 78% when compared to that of CKF. And for voltage phase angle, the mean of absolute errors using ISCKF is decreased to half that of using CKF. Alternatively, it can be said that the precision in the voltage phase angle estimation by ISCKF has been enhanced by 48% than that of CKF. (b) Absolute phase error percentage (APEP) and Absolute voltage error percentage (AVEP) [21] at a time instant are given as following:

$$APEP = \frac{100}{n_b - 1} \sum_{i=2}^{n_b} \frac{\hat{\theta}_i - \theta_i}{\theta_i} \qquad (31)$$

$$AVEP = \frac{100}{n_b} \sum_{i=1}^{n_b} \frac{\hat{V}_i - V_i}{V_i} \qquad (32)$$

where n_b is count of buses in system, $\hat{\theta}_i$, $\hat{V}_i$ are forecasted phase angle and voltage at bus respectively, θ_i, V_i are actual phase angle and voltage magnitude at bus.

It is also verified (from Table 4) with all the parameters mean, maximum and standard deviation of absolute phase error percentage (APEP) [21] and absolute voltage error percentage (AVEP) using ISCKF are less than that of CKF for IEEE 30-bus system.

Table 4. Absolute phase error percentage (APEP) and Absolute voltage error percentage (AVEP) comparison of proposed ISCKF with CKF methods for the two test systems (Note: SD stands for standard deviation and Max. for maximum).
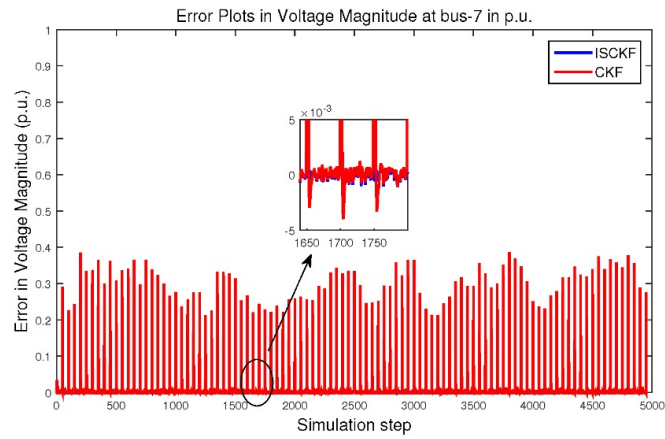
| | **IEEE 30-Bus System** | | | | | |
| | **APEP** | | | **AVEP** | | |
Filter Type	**Mean**	**Max.**	**SD**	**Mean**	**Max.**	**SD**
ISCKF	0.32	91.27	2.01	0.21	38.73	1.17
CKF	0.35	101.24	2.14	0.96	80.77	5.05
	NRPG 246-bus test system					
	APEP			**AVEP**		
Filter Type	**Mean**	**Max**	**SD**	**Mean**	**Max**	**SD**
ISCKF	0.01	1.33	0.03	0.02	33.22	0.97
CKF	0.03	1.78	0.08	0.80	66.28	4.53

- Execution time: It can be observed from the Table 3 that the ISCKF takes 15.93 ms whereas the CKF takes 7.43 ms. for execution of one hybrid data and 49 PMU data. It is evident that ISCKF is slightly slower than the CKF. However the data reporting time for hybrid measurement is 2 s, so ISCKF is able to give results before the next set of hybrid data arrives, which is expected from an estimation algorithm.
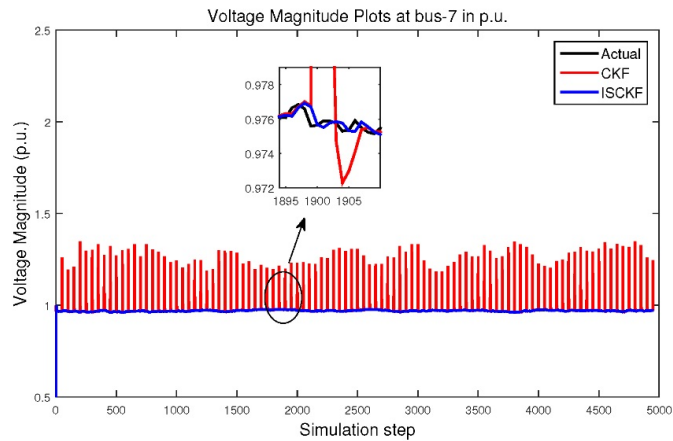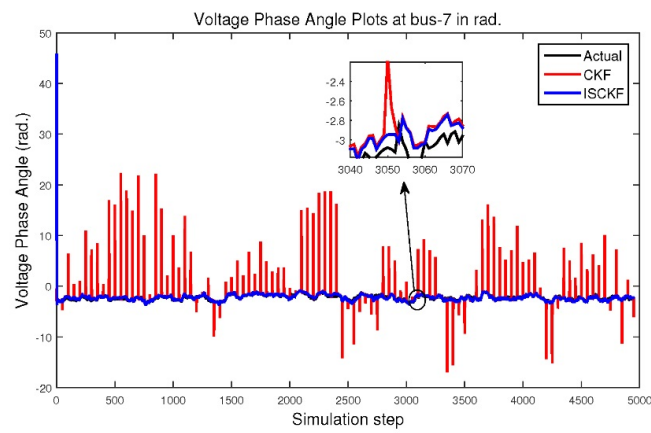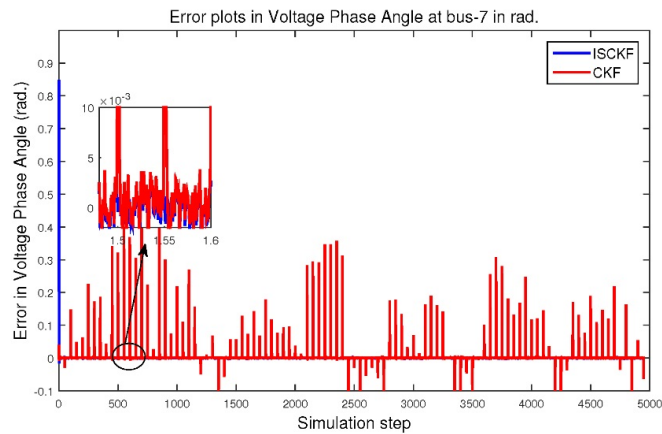

(a) Voltage Magnitude

Figure 3. *Cont.*

(b) Error in Voltage Magnitude

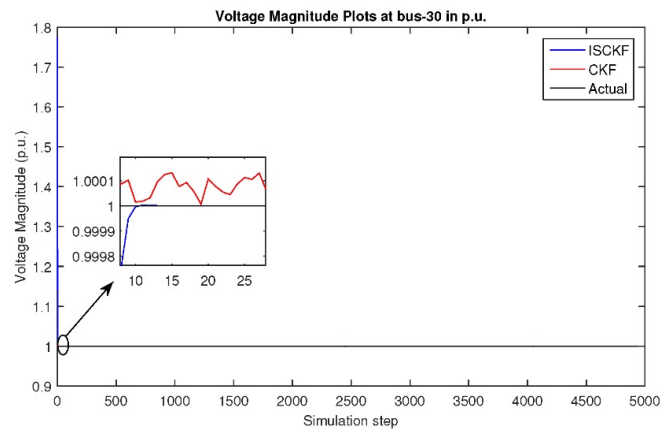**(c)** Voltage Phase angle

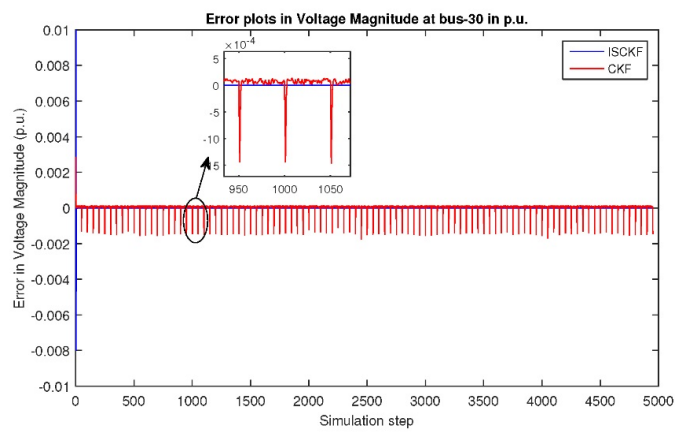**(d)** Error in Voltage Phase angle

Figure 3. The estimated states and error plots at bus-7 in IEEE 30-bus system.
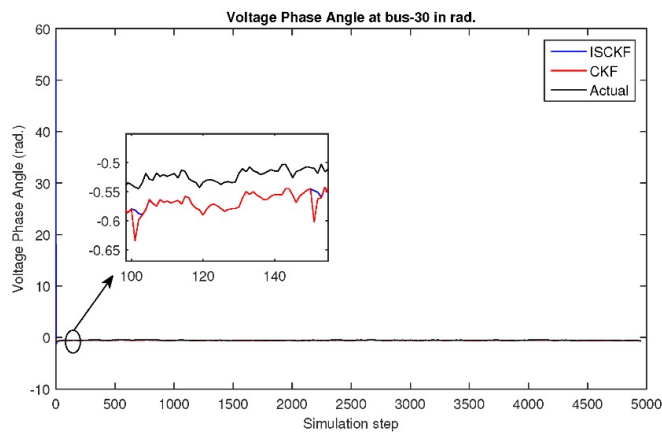
2. NRPG 246-bus system:

- For the comparison of ISCKF and CKF estimation results, actual data and estimation results consisting of voltage magnitude and voltage phase angle plots and their respective error plots at bus-30 are plotted in Figure 4. From Figure 4b,d, it is noticed that the estimation error using ISCKF is significantly less than that of using CKF.
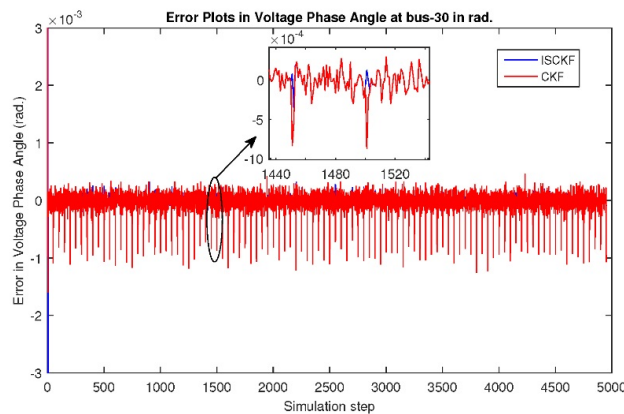
(**a**) Voltage Magnitude

(**b**) Error in Voltage Magnitude

(**c**) Voltage Phase angle

Figure 4. *Cont.*

(d) Error in Voltage Phase angle

Figure 4. The estimated states and error plots at bus-30 in NRPG 246-bus system.

- Error in estimation: (a) It is observed (Refer Table 2) that the mean of absolute error in voltage magnitudes at all buses is reduced to 1/16th that obtained using CKF. The precision in the voltage magnitude estimations by ISCKF is enhanced by approximately 94% than that of CKF. And the mean of absolute errors of voltage phase angle using ISCKF is decreased to 1/11th that of using CKF. Alternatively, it can be said that the accuracy in the voltage phase angle estimation by ISCKF has increased by 90% than that of CKF. (b) It is verified (from Table 4) with all the parameters mean, maximum and standard deviation of APEP and AVEP using ISCKF are less than that of CKF.

- Execution time: It can be observed from the Table 3 that the ISCKF takes 1.36 s whereas the CKF takes 0.84 s for execution of one hybrid data and 49 PMU data. It is evident that ISCKF is slower than the CKF. However the data reporting time for hybrid measurement is 2 s. So, ISCKF will be able to give results before the next set of hybrid data arrives (expected from an estimation algorithm). Therefore, the proposed estimation algorithm is applicable for real-time practical application, with respect to large power systems as well.

7. Conclusions

The paper demonstrates the deployment of an iterated square-root cubature Kalman filter for forecasting-aided state estimation during realistic load variations:

1. It is performed utilizing the hybrid measurements from both field devices: RTUs and PMUs.

2. The ISCKF method has the Newton-Gauss iterative method embedded into square-root CKF to improve its performance and stability. Consequently, ISCKF removes the risk of losing positive definiteness of the error covariance matrix in each update, which can cause the CKF to cease operating.

3. The online real-time application feasibility is demonstrated with respect to the two different sized test systems IEEE 30-bus and NRPG 246-bus systems.

4. The simulation results show that the proposed ISCKF outperforms the CKF by significant improvement in accuracy of forecasting-aided state estimation. This was evaluated with the help of mean of absolute errors, absolute phase error percentage and absolute voltage error percentage. For the voltage magnitude, the average estimation performance of ISCKF at all buses in system was in the range of 78%–94% increased accuracy when compared to that of CKF with respect to the 2 test systems considered. While for voltage phase angle, the increase was in the range of 48%–90% with respect to the 2 systems considered.

Future scope: In the dynamic state estimation studies for power systems, it is recommended that test cases be run against model uncertainty and cyber threats [37] for modern power systems.

Conflict of interest

There is no conflict of interest for this study.

Appendix

Table A1. Measurement quantities and corresponding standard uncertainties.

Measurement Device	Power Injection in p.u.	Line Flow in p.u.	V Magnitude in p.u.	V Angle rad.
RTU	0.01	0.01	0.006	-
PMU	0.001	0.001	0.0006	0.018

References

[1]   Z. B. Yang, D. X. Zhong, F. C. Guo, and Y. Y. Zhou, "Gauss-Newton iteration based algorithm for passive location by a single observer," *Syst. Eng. Electron.*, vol. 29, pp. 2006–2009, 2007.

[2]   G. Valverde, S. Chakrabarti, E. Kyriakides, and V. Terzija, "A Constrained Formulation for Hybrid State Estimation," *IEEE Trans. Power Syst.*, vol. 26, pp. 1102–1109, 2010, https://doi.org/10.1109/TPWRS.2010.2079960.

[3]   M. Asprou, E. Kyriakides, and M. Albu, "The Effect of Variable Weights in a WLS State Estimator Considering Instrument Transformer Uncertainties," *IEEE Trans. Instrum. Meas.*, vol. 63, pp. 1484–1495, 2013, https://doi.org/10.1109/TIM.2013.2292138.

[4]   R. Sodhi, S. C. Srivastava, and S. N. Singh, "Phasor-assisted Hybrid State Estimator," *Electr. Power Components Syst.*, vol. 38, pp. 533–544, 2010, https://doi.org/10.1080/15325000903376925.

[5]   M. Lixia, A. Benigni, A. Flammini, C. Muscas, F. Ponci, and A. Monti, "A Software-Only PTP Synchronization for Power System State Estimation With PMUs," *IEEE Trans. Instrum. Meas.*, vol. 61, pp. 1476–1485, 2012, https://doi.org/10.1109/TIM.2011.2180973.

[6]   M. Pau, P. A. Pegoraro, and S. Sulis, "Efficient Branch-Current-Based Distribution System State Estimation Including Synchronized Measurements," *IEEE Trans. Instrum. Meas.*, vol. 62, pp. 2419–2429, 2013, https://doi.org/10.1109/TIM.2013.2272397.

[7]   M. D. Kusljevic and P. D. Poljak, "Simultaneous Reactive-Power and Frequency Estimations Using Simple Recursive WLS Algorithm and Adaptive Filtering," *IEEE Trans. Instrum. Meas.*, vol. 60, pp. 3860–3867, 2011, https://doi.org/10.1109/TIM.2011.2144690.

[8]   A. Sharma, S. C. Srivastava, and S. Chakrabarti, "A Cubature Kalman Filter Based Power System Dynamic State Estimator," *IEEE Trans. Instrum. Meas.*, vol. 66, pp. 2036–2045, 2017, https://doi.org/10.1109/TIM.2017.2677698.

[9]   J. Zhao et al., "Power System Dynamic State Estimation: Motivations, Definitions, Methodologies, and Future Work," *IEEE Trans. Power Syst.*, vol. 34, pp. 3188–3198, 2019, https://doi.org/10.1109/TPWRS.2019.2894769.

[10]   P. Rousseaux, D. Mallieu, T. Van Cutsem, and M. Ribbens-Pavella, "Dynamic state prediction and hierarchical filtering for power system state estimation," *Automatica*, vol. 24, pp. 595–618, 1988, https://doi.org/10.1016/0005-1098(88)90108-2.

[11]   H. Beides and G. Heydt, "Dynamic state estimation of power system harmonics using Kalman filter methodology," *IEEE Trans. Power Del.*, vol. 6, pp. 1663–1670, 1991, https://doi.org/10.1109/61.97705.

[12] A. Sinha and J. Mondal, "Dynamic state estimator using ANN based bus load prediction," *IEEE Trans. Power Syst.*, vol. 14, pp. 1219–1225, 1999, https://doi.org/10.1109/59.801876.

[13] M. Huang, Z. Wei, and Y. Lin, "Forecasting-aided state estimation based on deep learning for hybrid AC/DC distribution systems," *Appl. Energy*, vol. 306, p. 118119, 2021, https://doi.org/10.1016/j.apenergy.2021.118119.

[14] J. -M. Lin, S. -J. Huang, and K. -R. Shih, "Application of sliding surface-enhanced fuzzy control for dynamic state estimation of a power system," *IEEE Trans. Power Syst.*, vol. 18, pp. 570–577, 2003, https://doi.org/10.1109/TPWRS.2003.810894.

[15] N. R. Shivakumar and A. Jain, "A Review of Power System Dynamic State Estimation Techniques," in *Proc. 2008 Joint Int. Conf. Power Syst. Technol. and IEEE Power India Conf. (POWERCON)*, New Delhi, India, 2008, https://doi.org/10.1109/ICPST.2008.4745312.

[16] J. Mandal, "Incorporating nonlinearities of measurement function in power system dynamic state estimation," *IEE Proc. C Gener. Transm. Distrib.*, vol. 142, p. 289, 1995, https://doi.org/10.1049/ip-gtd:19951715.

[17] A. Bahgat, M. Sakr, and A. El-Shafei, "Two level dynamic state estimator for electric power systems based on nonlinear transformation," *IEE Proc. C Gener. Transm. Distrib.*, vol. 136, pp. 15–23, 1989, https://doi.org/10.1049/ip-c.1989.0003.

[18] I. Ferreira and F. M. Barbosa, "A square root filter algorithm for dynamic state estimation of electric power systems," in *Proc. MELECON'94. Mediterr. Electrotechnica. Conf.*, Antalya, Turkey, 1994, https://doi.org/10.1109/MELCON.1994.380962.

[19] A. Jain and N. R. Shivakumar, "Impact of PMU in dynamic state estimation of power systems," in *Proc. 2008 40th North Am. Power Symp.*, Calgary, AB, Canada, 2008, https://doi.org/10.1109/NAPS.2008.5307352.

[20] H. Li and W. Li, "Estimation and forecasting of dynamic state estimation in power systems," in *Proc. 2009 Int. Conf. Sustain. Power Gener. Supply*, Nanjing, China, 2009, https://doi.org/10.1109/SUPERGEN.2009.5348376.

[21] C. Gu and P. Jirutitijaroen, "Dynamic State Estimation Under Communication Failure Using Kriging Based Bus Load Forecasting," *IEEE Trans. Power Syst.*, vol. 30, pp. 2831–2840, 2015, https://doi.org/10.1109/TPWRS.2014.2382102.

[22] G. Valverde and V. Terzija, "Unscented Kalman Filter for Power System Dynamic State Estimation," *IET Gener. Transm. Distrib.*, vol. 5, pp. 29–37, 2011, https://doi.org/10.1049/iet-gtd.2010.0210.

[23] Y. Yang, W. Hu, and Y. Min, "Projected unscented Kalman filter for dynamic state estimation and bad data detection in power system," in *Proc. 12th IET Int. Conf. Developments in Power Syst. Protection (DPSP 2014)*, Copenhagen, Denmark, 2014, https://doi.org/10.1049/cp.2014.0109.

[24] M. Hassanzadeh and C. Y. Evrenosoglu, "A regression analysis based state transition model for power system dynamic state estimation," in *Proc. 2011 North American Power Symp.*, Boston, MA, USA, 2011, https://doi.org/10.1109/NAPS.2011.6024897.

[25] M. Nejati, N. Amjady, and H. Zareipour, "A New Stochastic Search Technique Combined With Scenario Approach for Dynamic State Estimation of Power Systems," *IEEE Trans. Power Syst.*, vol. 27, pp. 2093–2105, 2012, https://doi.org/10.1109/TPWRS.2012.2195038.

[26] H. Zhao and B. Tian, "Robust Power System Forecasting-Aided State Estimation With Generalized Maximum Mixture Correntropy Unscented Kalman Filter," *IEEE Trans. Instrum. Meas.*, vol. 71, pp. 1–10, 2022, https://doi.org/10.1109/TIM.2022.3160562.

[27] Z. Zhang, Z. Zhang, S. Zhao, Q. Li, Z. Hong, F. Li, and S. Huang, "Robust adaptive Unscented Kalman Filter with gross error detection and identification for power system forecasting-aided state estimation," *J. Frankl. Inst.*, vol. 360, pp. 10297–10336, 2023, https://doi.org/10.1016/j.jfranklin.2023.07.022.

[28] N. Veerakumar, D. Ćetenović, K. Kongurai, M. Popov, A. Jongepier, and V. Terzija, "PMU-based Real-time Distribution System State Estimation Considering Anomaly Detection, Discrimination and Identification," *Int. J. Electr. Power Energy Syst.*, vol. 148, p. 108916, 2023, https://doi.org/10.1016/j.ijepes.2022.108916.

[29] S. Wei, Z. Wu, J. Xu, and Q. Hu, "Multiarea Probabilistic Forecasting-Aided Interval State Estimation for FDIA Identification in Power Distribution Networks," *IEEE Trans. Ind. Inform.*, vol. PP, pp. 1–12, 2023, https://doi.org/10.1109/TII.2023.3321098.

[30] I. Arasaratnam and S. Haykin,"Cubature Kalman Filters,"*IEEE Trans. Autom. Control.*, vol. 54, pp. 1254–1269, 2009, https://doi.org/10.1109/TAC.2009.2019800.

[31] C. Wang, P. Wu, and Y. Deng,"Modified iterated square-root cubature Kalman filter for non-cooperative space target tracking,"*Int. J. Appl. Sci. Eng.*, vol. 2, p. 257789, 2015.

[32] A. L. da Silva, M. D. C. Filho, and J. de Queiroz,"State forecasting in electric power systems,"*IEE Proc. C Gener. Transm. Distrib.*, vol. 130, pp. 237–244, 1983, https://doi.org/10.1049/ip-c.1983.0046.

[33] A. Abur and A. G. Exposito, *Power System State Estimation: Theory and Implementation*. Boca Raton, FL, USA: CRC Press, 2004.

[34] R. D. Zimmerman, C. E. Murillo-Sanchez, and R. J. Thomas,"MATPOWER: Steady-State Operations, Planning, and Analysis Tools for Power Systems Research and Education,"*IEEE Trans. Power Syst.*, vol. 26, pp. 12–19, 2010, https://doi.org/10.1109/TPWRS.2010.2051168.

[35] M. Shahidehpour and Y. Wang,"Appendix C: IEEE30 bus system data,"in *Communication and Control in Electric Power Systems: Applications of Parallel and Distributed Processing*, Piscataway, NJ, USA: Wiley-IEEE Press, 2004, pp. 493–495.

[36] "246 Bus Reduced NRPG System Data,"Accessed: Sep. 13, 2023. [Online]. Available: https://www.iitk.ac.in/eeold/facilities/Research%20labs/Power%20System/NRPG-DATA.pdf.

[37] J. Qi, A. F. Taha, and J. Wang,"Comparing Kalman Filters and Observers for Power System Dynamic State Estimation With Model Uncertainty and Malicious Cyber Attacks,"*IEEE Access*, vol. 6, pp. 77155–77168, 2018, https://doi.org/10.1109/ACCESS.2018.2876883.